Competitive halogenation of silicon surfaces in HBr/Cl_2 plasmas studied with x-ray photoelectron spectroscopy and *in situ*, real-time, pulsed laser-induced thermal desorption

C. C. Cheng,[a] K. V. Guinn, I. P. Herman,[b] and V. M. Donnelly
AT&T Bell Laboratories, Murray Hill, New Jersey 07974

(Received 18 October 1994; accepted 11 March 1995)

Using x-ray photoelectron spectroscopy (XPS) and real-time, laser-induced thermal desorption–laser-induced fluorescence (LD–LIF), we have determined the coverage of Br and Cl on Si(100) surfaces that are etched in mixed HBr/Cl_2 plasmas. Halogen coverages measured by XPS after etching are directly proportional to the fraction of the respective halogen in the feed gas. LD–LIF was detected from $SiCl_{(g)}$ and $SiBr_{(g)}$ products with intensities that are a semiquantitative measure of instantaneous Cl and Br coverages. Saturated coverages during etching in Cl_2 and HBr plasmas are 1.0×10^{15} Cl/cm^2 and 6.0×10^{14} Br/cm^2, respectively. Etch rates at these two extremes are 2170 and 1330 Å/min, and therefore are proportional to the respective halogen coverages. It therefore appears that the rate of formation of volatile Si–halides, stimulated by ion bombardment, is lower for HBr mainly because less halogen is available on the surface at saturated coverage. Langmuir probe measurements indicate that the ion flux is 17% lower in pure HBr plasmas, compared with Cl_2 plasmas at the same power. The plasma potential, direct current bias voltage, and hence ion energy were nearly constant, however, over the range of gas mixtures. The slightly different ion fluxes suggest that the ion bombardment-stimulated process, although similar for Cl_2 and HBr plasmas, is actually slightly more efficient on a per halogen basis for Br versus Cl. Positive photoresist surfaces that were also exposed to the plasma differ from Si in that less Br adsorbs on the surface both in pure HBr and mixed HBr/Cl_2 plasmas. Apparently the lower reactivity of photoresist with Br (compared with Cl) is at least partly responsible for the widely observed slower etch rate of photoresist in HBr plasmas, and hence enhanced selectivity when etching Si. © *1995 American Vacuum Society.*

I. INTRODUCTION

Virtually all plasma etching processes for Si involve the formation of volatile Si–halide products.[1–3] Fluorine-containing plasmas are usually avoided because, although high etch rates can be obtained, the fast chemical reaction with F atoms leads to undercutting of the mask and thus a loss of anisotropy.[1–4] Cl atoms etch Si very slowly (except for n^+ doped) in the absence of ion bombardment,[5] while etching with Cl and Cl_2 is greatly accelerated by ion bombardment.[3,6] Consequently, Cl-containing plasmas are widely used for anisotropic etching of Si. Cl-containing plasmas do, however, have some disadvantages. Etched profiles often deviate from ideal vertical sidewalls, and selectivity with respect to etching of SiO_2 and especially photoresist etch masks is often not as high as desired. Br-containing plasmas (e.g., HBr feed gas) have been reported to have superior anisotropy and selectivity for etching of Si.[7–15] In general, etch rates are not as high as those in Cl_2 plasmas, however, and consequently many etch processes have been developed with a mixture of Cl_2 and HBr to simultaneously obtain high rates and selectivities, and nearly ideal anisotropy. The mechanisms by which simultaneous impingement by Cl, Br, and H-containing species affects the Si etch rate, etch profile, and selectivity are unknown.

Previously, we reported a technique for real-time detection of adsorbates during plasma etching in which laser-induced desorption (LD) was combined with laser-induced fluorescence (LIF) detection.[16,17] Chlorine coverage was determined during etching of Si in high density, low pressure helical resonator plasmas of pure Cl_2 and Cl_2/O_2 for a range of plasma conditions, using LD–LIF detection of SiCl. Coupled with x-ray photoelectron spectroscopy (XPS) after sample transfer under high vacuum, it was shown that Cl coverage scaled with the SiCl LD–LIF signal. The Cl coverage during etching was found to be about twice the saturated Cl coverage obtained by exposing Si to Cl_2 in the absence of a plasma. The Cl coverage did not change appreciably after the plasma was extinguished and the gas was pumped away. At pressures above ~0.5 mTorr, the layer formed during etching reached saturated coverage on a time scale that was short compared to the etch rate. From the pressure, power, and direct current (dc) bias dependences we concluded that ion flux limits the rate of desorption of etch products, and therefore also the etch rate, even in these low pressure, high-charge-density plasmas.

In the present study, we extend the LD–LIF method to study Si(100) surfaces in real time during etching in mixed HBr/Cl_2 plasmas. Cl and Br coverages were monitored by LD–LIF detection of SiCl and SiBr, respectively. XPS analysis was also performed after etching to measure Cl and Br coverages on Si(100), as well as on polycrystalline-Si (poly-Si) and photoresist surfaces.

---

[a] Present address: Gasonics International, 2730 Junction Ave., San Jose, CA 95134-1909.

[b] Also at the Department of Applied Physics and the Columbia Radiation Laboratory, Columbia University, New York, NY 10027.

II. EXPERIMENTAL PROCEDURE

The apparatus used in this study has been described in detail in recent publications.[16–19] The helical resonator plasma reactor is connected to an ultrahigh vacuum (UHV) XPS analysis chamber by a high-vacuum sample transfer chamber. The discharge was operated with a mixture of HBr and Cl_2 at a total pressure of 2.1 mTorr [see Ref. 20(a) for a correction of pressures in previous studies] and at a constant total flow of 5.5 standard cubic centimeters per minute (sccm). The helical resonator source was operated at a radio frequency (rf) of 11.21 MHz and a net power of 280 W, and the substrate stage was biased with a second rf (14.5 MHz) source, to obtain a dc bias voltage of −35 V. Si(100) substrates (n type, P doped, 5–50 Ω cm) were cleaved into 1.5×1.5 cm pieces and clamped to a 1 in. diam. stainless steel sample holder that can be transferred under high vacuum from the etching chamber to the analysis chamber. The wafer temperature was measured directly by interferometric thermometry, as described elsewhere.[18,19] The sample temperature, initially at 25 °C, increased to 130 °C in 3 min and ~200 °C in 6 min. Most of the measurements reported here required that the plasma be on <3 min. No changes in signals were observed that could be ascribed to heating of the wafer during longer plasma exposures.

During etching, the Si(100) surface was irradiated with laser pulses and laser-desorbed SiCl and SiBr products were detected by laser-induced fluorescence. The XeCl excimer laser (Lambda Physics model EMG 203, $\lambda=308$ nm) was operated at 5 Hz and delivered a fluence of 0.47 J/ cm^2 to the sample surface at normal incidence in a 2.6×6.2 mm rectangular beam. LIF was dispersed with a monochromator and detected with a GaAs photomultiplier tube. Lenses were used to image light from the near-surface region (0–4 mm above the surface) onto the entrance slit of the monochromator. A boxcar integrator with a 1-μs-wide gate was used to integrate over the signal pulse generated by the 15-ns-long laser pulse.

After etching and transfer of the sample to the analysis chamber, XPS analysis was performed on Si(100), undoped poly-Si, and photoresist surfaces. The photoresist was a positive resist (Shipley 1805) composed of 30 wt % novolac resin and 70 wt % 1-oxo-2-diazo-napthoquinone-5-arylsulfonate sensitizer. The atomic composition of this mixture (excluding H) is: 83% C, 14% O, 2% N, and 1% S.

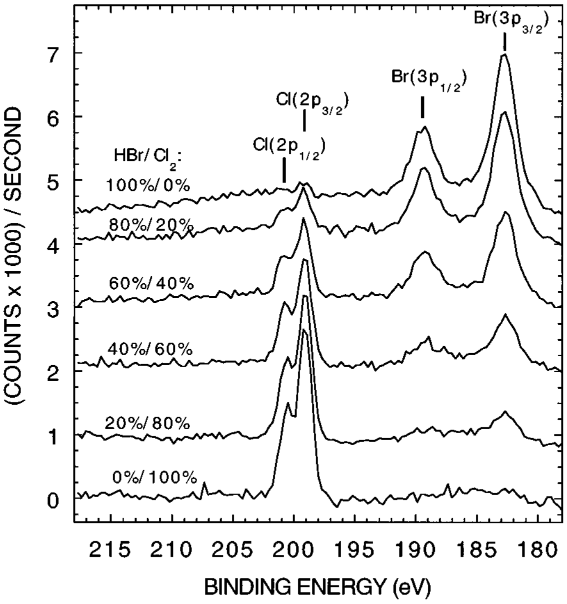

FIG. 1. XPS spectra of Cl($2p$) and Br($3p$) on Si(100), recorded after etching in HBr/Cl_2 plasmas. The top five spectra have their intensities offset for clarity. Br($3p$) lines are presented here because they are close in binding energy to the Cl($2p$) line. The Br($3d$) line is used in subsequent analysis [Ref. 20(b)].

III. RESULTS

Typical Br($3p$) and Cl($2p$) XPS spectra are shown in Fig. 1 for Si(100) after etching with different HBr:Cl_2 ratios. As expected, both Br and Cl are adsorbed on Si(100) after etching in HBr/Cl_2 plasmas, and the XPS signal increases with increasing proportion of the respective halogen in the feed gas. Small Br($3p$) and Cl($2p$) signals in pure Cl_2 and HBr plasmas, respectively, are due to residual HBr (and possibly Br_2) and Cl_2 desorbing from the walls of the chamber. XPS measurements performed on poly-Si surfaces (not shown in the figures, but included in Table I) were indistinguishable from the Si(100) results, as may be expected, since ion bombardment would likely make both these surfaces disordered.[21]

LD–LIF spectra are shown in Fig. 2 for feed gas ratios spanning those used in the XPS measurements presented in Fig. 1. Background from scattered laser light has been sub-

TABLE I. Etch rates and halogen coverages for etching of poly-Si and photoresist in HBr/Cl_2 plasmas. Cl and Br coverages are Cl($2p$) and Br($3d$) XPS integrated peak intensities, corrected for sensitivity differences, and normalized to Si($2p$) (for poly-Si) and C($1s$) (for photoresist) XPS signals, also normalized for sensitivity differences. Uncertainties are ±7% in poly-Si etch rates, ±20% in photoresist etch rates, and ±5% in Cl and Br coverages.

	poly-Si			Photoresist		
%HBr/%Cl_2	Etch rates (Å/min)	Cl	Br	Etch rates (Å/min)	Cl	Br
0/100	2166	0.48	⋯	2320	0.50	⋯
20/80	2498	0.40	0.045	1630	0.40	0.019
100/0	1334	⋯	0.30	628	⋯	0.21

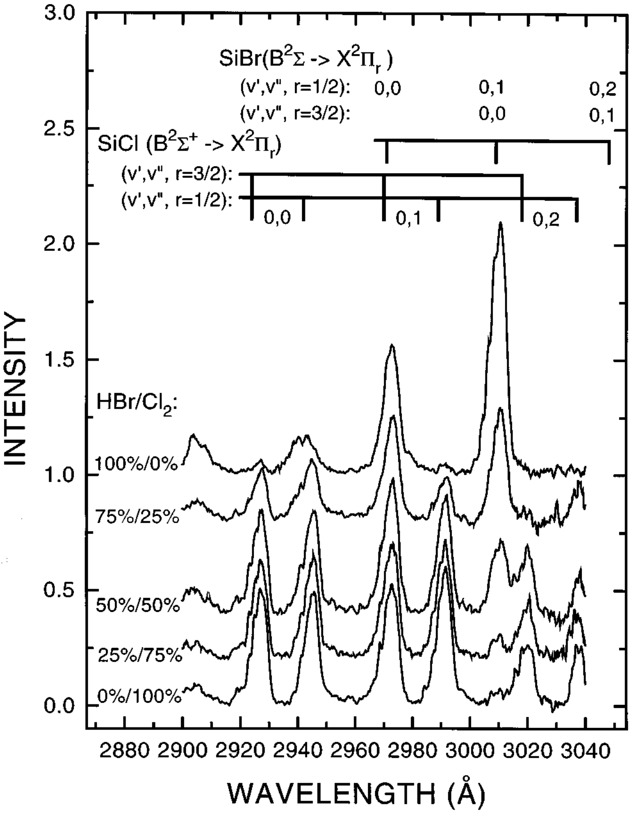

FIG. 2. Laser-desorption, laser-induced fluorescence spectra recorded during etching of Si(100) in HBr/Cl_2 plasmas. The background scattered laser light has been subtracted from the spectra, and the intensities of all but the bottom spectrum have been offset for clarity. The bandheads for SiCl and SiBr emission are indicated in the upper area.

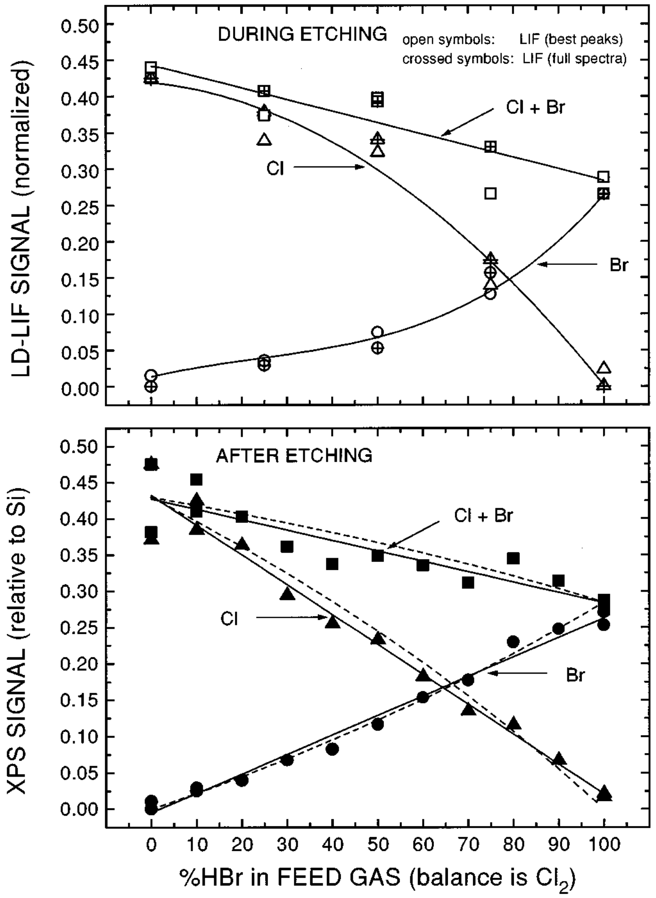

FIG. 3. Bottom: Cl(2*p*) (▲), Br(3*d*) (●), and Cl(2*p*)+Br(3*d*) (■) XPS integrated peak intensities [normalized to Si(2*p*) and corrected for sensitivity differences], recorded after etching in HBr/Cl_2 plasmas, as a function of % HBr. The solid lines are linear least square fits. The dashed lines are predicted dependences if Br and Cl compete equally for adsorption sites, in proportion to the halogen content of the feed gas. Top: SiCl (△), SiBr (○), and SiCl+SiBr (□) LIF intensities [normalized to the corrected Cl(2*p*) and Br(3*d*) XPS intensities at 100% Cl_2 and HBr, respectively] vs % HBr. The open symbols refer to intensities derived from single peaks (2989 Å for SiCl and 3009 Å for SiBr), and the open, crossed symbols refer to signals derived from a least squares fit to a combination of spectra for pure Cl_2 and HBr plasmas. The curves, which are second- and third-order polynomial fits, are to guide the eye.

tracted from raw spectra to obtain the traces shown in Fig. 2. In a Cl_2 plasma, LD–LIF occurs as a two-step process in which a single laser pulse heats the surface near or to the melting point (1410 °C), causing desorption of $SiCl_x$ product. The tail of the same laser pulse promotes a fraction of the desorbed species into an electronically excited state that subsequently fluoresces. The emitter was previously identified as $\mathrm{SiCl}(B\,^2\Sigma^+)$,[16,17] excited within a distance of $\sim 10\ \mu$m of the surface by a resonance at 308 nm with the transitions:

$$\mathrm{SiCl}(B\,^2\Sigma^+)(\nu'=0)\leftarrow\mathrm{SiCl}(X\,^2\Pi_{3/2,1/2})(\nu''=3,4). \tag{1}$$

An analogous LD–LIF process occurs during etching of Si in a pure HBr plasma. The emitter is $\mathrm{SiBr}(B\,^2\Sigma^+)$,[22,23] excited at 308 nm as a result of the transitions:

$$\mathrm{SiBr}(B\,^2\Sigma^+)(\nu'=0)\leftarrow\mathrm{SiBr}(X\,^2\Pi_{3/2,1/2})(\nu''=1-3) \tag{2}$$

Fluorescence from the excited state to the $\nu''=0$, 1 levels of the ground electronic state is readily identified in the top spectrum in Fig. 2, recorded during etching in a pure HBr plasma. LD–LIF spectra for mixed HBr/Cl_2 plasmas contain contributions from both SiBr and SiCl that scale with the fraction of the respective halogen in the feed gas, similar to the XPS spectra in Fig. 1.

The integrated XPS peak intensities for Cl(2*p*), Br(3*d*) and Cl(2*p*)+Br(3*d*) are presented in Fig. 3.[20(b)] The intensities are divided by XPS sensitivity factors and ratioed to the integrated Si(2*p*) peak intensity, which is also divided by its sensitivity factor. Consequently, relative coverages of Cl can be compared to those for Br by comparing the XPS intensities plotted in Fig. 3. The solid lines are linear least-square fits to the data. Br signal (and hence coverage) increases in proportion to the percentage of HBr in the input gas mixture. Similarly, Cl coverage is directly proportional to the amount of Cl_2 in the feed gas. The Cl coverage after etching in a pure Cl_2 plasma is 1.6 times higher than the Br coverage measured after etching in a pure HBr plasma. The dashed, slightly curved lines represent halogen coverages that are proportional to the fraction of halogen contained in the feed gas, and will be described in more detail.

Integrated intensities for SiCl, SiBr, and SiCl+SiBr LD–LIF are also presented in Fig. 3. Two methods of analysis were used. First, the best peak with minimum "crosstalk" was chosen for SiCl (2989 Å) and SiBr(3009 Å). Second, the spectra for 100% HBr and 100% Cl_2 were used as "func-

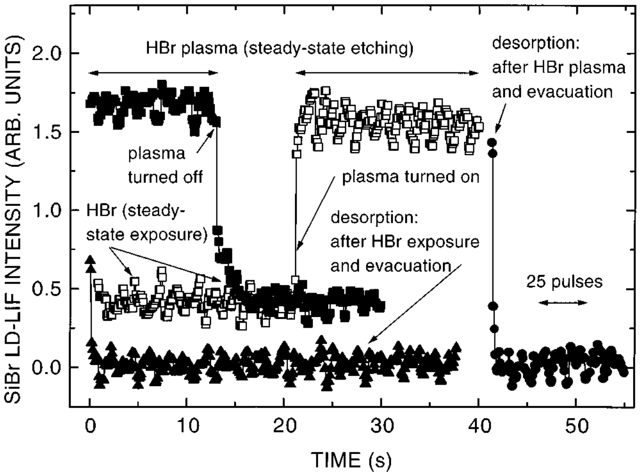

FIG. 4. Time dependence of the SiBr LD–LIF signal intensity during (■,□) and after (●,▲) plasma etching or gas exposure of Si(100) in pure HBr.

tions'' and the remaining three spectra for mixed HBr/Cl$_2$ plasmas were used in least square fits generated from a mixture of these two functions. The results of both methods of analysis are presented in Fig. 3. The agreement between the two methods is acceptable, indicating that the entire SiCl and SiBr spectra have the same dependence on %HBr. Although the SiCl and SiBr LD–LIF signals depend on %HBr in a manner that is qualitatively similar to the Cl$(2p)$ and Br$(3d)$ XPS signals, the SiBr signal (normalized to the Br–XPS signal at 100% HBr) drops below the Br coverage measured by XPS for mixed HBr/Cl$_2$ plasmas. Conversely, the SiCl LD–LIF signal (normalized to the Cl–XPS signal for pure Cl$_2$ plasmas) is higher on average than the Cl XPS coverage after etching in HBr/Cl$_2$ mixtures. The total SiBr+SiCl LD–LIF signal is, however, in agreement with the total Br+Cl coverage determined from XPS.

The time dependence and stability of the SiBr$_x$ adsorbed layer after etching in an HBr plasma (Fig. 4) was investigated in the same manner as that reported previously for the SiCl$_x$ layer after etching in a Cl$_2$ plasma.[16,17] After the steady-state signal was established during etching, the plasma was turned off while the laser continued to irradiate the surface (■ in Fig. 4). The signal immediately (with 1 laser pulse) dropped by a factor of 2 and then decayed by another ~30% over the next 20 laser pulses. The steady-state signal level with no plasma is about one-fourth of the intensity observed during plasma exposure, and indicates a significant amount of laser-induced etching. The trend is reversible, as shown by the open square symbols.

In another experiment, steady-state plasma etching is established, the laser is blocked *before* the plasma is extinguished, the gas is pumped away, and the laser is unblocked. The signal on the first laser pulse is equal to the steady-state signal and decays to baseline within a few pulses. This indicates that the SiBr$_x$ layer is stable after the plasma is extinguished. Consequently, surface analysis carried out after etching and then transferring the sample to the analysis chamber under vacuum is representative of the surface that was present during etching.[15–19] A similar observation and conclusion have been made for the layer present during and after exposure to HBr with the plasma off (▲ in Fig. 4). All of these time-dependent results are analogous to observations for the SiCl$_x$ layer formed by etching Si in a Cl$_2$ plasma.[16,17]

Etch rates for poly-Si and photoresist were determined for pure Cl$_2$ and HBr plasmas, and for one mixture (20%HBr/80%Cl$_2$). These results are summarized in Table I, along with XPS measurements of Cl and Br coverages (normalized to the major component of the underlying material).

Previous Langmuir probe measurements of pure Cl$_2$ plasmas indicated that the positive ion flux was 4×10^{16} cm^{-2} s^{-1}, and the plasma potential was 50 V.[17] These measurements were reproduced in the present study, and additional measurements of mixed HBr/Cl$_2$ plasmas indicated that the ion flux fell by 17% between pure Cl$_2$ and 50% HBr/50%Cl$_2$ and then remained constant as the percentage of Cl$_2$ was further reduced. The plasma potential was constant to within 5 V over the range of gas mixtures.

IV. DISCUSSION

The saturated coverage of Cl, θ^0_{Cl}, measured by XPS after etching Si in a Cl$_2$ plasma was previously estimated to be 1.0×10^{15} cm^{-2}.[17] Based on the Cl-to-Br XPS ratio of 1.6:1 measured in the present study, we therefore estimate that the saturated Br coverage (θ^0_{Br}) is 6.0×10^{14} cm^{-2} after etching in HBr plasmas. The lower Br coverage is likely due in part to site blocking by coadsorbed H. Although we could not determine H coverages in this study, H atoms are present in the discharge and therefore are expected to adsorb on the surface during etching. In addition, adjacent adsorption sites could be blocked by the larger Br atom (atomic radii of Cl and Br are 0.97 and 1.12 Å, respectively). This steric hindrance is expected to be more effective in suppressing di- and trihalide species that form during plasma etching and is consistent with observations (SiCl:SiCl$_2$:SiCl$_3$ =1.0:0.84:0.25, (SiBr:SiBr$_2$:SiBr$_3$=1.0:0.78:0.17).[15,17]

The dashed curves in Fig. 3 represent a simple model in which the halogen coverage is assumed to be proportional to the fraction of the respective halogen, f_{Br} and f_{Cl} in the feed gas, defined as

$$f_{\mathrm{Br}}=p_{\mathrm{HBr}}/(p_{\mathrm{HBr}}+2p_{\mathrm{Cl}_2}), \tag{3}$$

and

$$f_{\mathrm{Cl}}=2p_{\mathrm{Cl}_2}/(p_{\mathrm{HBr}}+2p_{\mathrm{Cl}_2}), \tag{4}$$

where p_{HBr} and p_{Cl_2} are the partial pressures of HBr and Cl$_2$. In addition, it is assumed that Br (plus any adsorbed H) occupies 1.6 times as many sites as Cl (the ratio of the reciprocals of the Br and Cl XPS coverages, θ^0_{Br} and θ^0_{Cl}, determined from pure HBr and Cl$_2$ experiments) for all gas ratios, and that the surface is always at saturated coverage during (and after) etching. So

$$\theta^0_{\mathrm{Cl}}=1.6\theta_{\mathrm{Br}}+\theta_{\mathrm{Cl}}, \tag{5}$$

where θ_{Br} and θ_{Cl} are the halogen coverage for etching in mixed HBr/Cl$_2$ plasmas. Therefore

$$\theta_{\mathrm{Br}}=\frac{\theta^0_{\mathrm{Cl}}\,f_{\mathrm{Br}}}{1+0.6f_{\mathrm{Br}}}. \tag{6}$$

The halogen coverages θ_{Br}, θ_{Cl}, and $\theta_{Br}+\theta_{Cl}$ computed from Eqs. (5) and (6) are plotted as the dashed lines in Fig. 3. Within the scatter of the data they provide good fits, indicating that the coverages determined by XPS for either halogen are simply proportional to the percentage of that halogen in the feed gas.

Contrary to the XPS data, when the LD–LIF signals are normalized to the XPS data at 0% and 100% HBr, for mixed HBr/Cl_2 plasmas the SiBr LD–LIF signal falls below the near-linear dependence on %HBr and Br (XPS) coverage, while the SiCl LD–LIF signal lies above the near-linear dependence on %Cl_2 and Cl (XPS) coverage. Either Br displaces Cl in the short period following etching, before the etching chamber is evacuated and the sample transferred to the analysis chamber, or the LD–LIF signals are not precisely proportional to the respective halogen coverages during etching.

To investigate the likelihood of Cl displacement by Br after plasma etching, the following additional measurements were performed. The Si sample was etched in a pure Cl_2 plasma for several minutes. The plasma was then extinguished and the Cl_2 pumped away. The reactor was then filled with HBr to a pressure of 2.1 mTorr for 1 min. The HBr was then pumped away and the sample was transferred to the XPS chamber. The Br coverage was only slightly higher than the trace amount observed after simply etching in a pure Cl_2 plasma, indicating that displacement of adsorbed Cl by Br from exposure to HBr, does not occur to any appreciable extent. The converse is also true; Cl does not displace adsorbed Br after etching in an HBr plasma and then exposing the sample to Cl_2.

Therefore, the relative halogen coverages measured by XPS after etching are expected to be close to those present during etching, and the LD–LIF signals deviate somewhat from these coverages. The dependence of the SiBr LD–LIF signal on Br XPS coverage could simply indicate that the relative yield of the SiBr laser-induced thermal desorption (LITD) increases as Br coverage increases, perhaps due to a weakening of the surface binding energy from repulsive adsorbate-adsorbate interactions. Previously we showed that the SiCl LD–LIF signal scaled linearly with Cl coverage measured by XPS when Cl coverage was changed from half of saturated coverage to saturated coverage.[16,17] The nonlinear dependence of the SiCl LD–LIF signal on Cl XPS coverage found in the present study is at odds with this observation. Formation and desorption of higher Si chlorides at saturated coverage is one possible explanation, but it is not clear why this behavior would be opposite to that found with adsorbed Br.

Perhaps a more likely explanation of both the Br and Cl results is a ‘‘matrix effect’’ in which adsorbed Cl suppresses desorption of SiBr, and to a lesser extent, adsorbed Br (and/or H) enhances SiCl desorption. LITD studies of Cl_2-dosed Si have shown that a large amount of $SiCl_2$ desorbs,[24] in addition to SiCl.[25–29] Thermal desorption studies have shown that $SiCl_2$ is probably the major product,[24,30,31] but that SiCl desorption begins to become important at higher temperatures if Cl_2 is continuously supplied to the surface.[32,33] Apparently, no measurements have been reported for LITD after exposing Si to HBr or Br_2. Thermal desorption studies find that the mass spectrum of the $SiBr_x$ product(s) favors $SiBr^+$ over $SiBr_2^+$ by 5:1.[34,35] These studies assume that this is the cracking pattern for $SiBr_2$, because the $SiBr^+$-to-$SiBr_2^+$ ratio changes little with desorption temperature.[34,35] It is possible that some of the $SiBr^+$ signal could be due to desorption of SiBr. In the present study, we show by LIF that SiBr is at least a minor product of LITD. LITD would be expected to enhance SiBr yields over those in thermal desorption, because high peak temperatures are reached.

One possible matrix effect leading to a smaller-than-expected SiBr LD–LIF signals involves the desorption of Si interhalides. The free energies of formation (ΔG_f) of SiCl and SiBr from $Si_{(s)}$ and the diatomic halogen gases are about the same (4.5 and -1.3 kcal/mol, respectively, at 1400 °C), while formation of $SiCl_2$ ($\Delta G_f = -53.7$ kcal/mol) is favored over $SiBr_2$ ($\Delta G_f = -31.4$ kcal/mol) at 1400 °C.[36] Thermodynamic constants for SiClBr are unknown, but are likely to be between those for $SiCl_2$ and $SiBr_2$. If LITD of $SiBr_2$ is less favored in HBr plasma etching than is $SiCl_2$ desorption in Cl_2 plasmas, then in HBr/Cl_2 plasmas desorption of SiClBr could deplete the surface of Br faster than does $SiBr_2$ desorption. Consequently, as the surface reaches its peak temperature where desorption of SiBr is expected to be most favored, the Br coverage would drop and so the yield of desorbed SiBr would decrease. Conversely, adsorbed Br could hinder formation and prompt desorption of $SiCl_2$ during the laser pulse, thereby enhancing the SiCl yield by providing more adsorbed Cl at the peak temperature. Regardless of the explanation for the small differences between the Si–halide LD–LIF signals and halogen coverages measured by XPS, the LD–LIF signals provide an instantaneous measure of Cl and Br coverages, which are accurate to within a factor of 1.7 for Br and 1.3 for Cl.

Because halogen coverage is proportional to the fraction of halogen in the feed gas, the overall rate of bromination in HBr plasmas, which is a function of the sticking coefficients and partial pressures of HBr, Br, Br_2, and Br-containing ions, must be nearly equal to the rate of chlorination in Cl_2 plasmas, which likewise depends on Cl_2, Cl, Cl_2^+, and Cl^+ sticking coefficients and partial pressures. Since it was shown previously that Si etching in a Cl_2 plasma is limited by ion bombardment and not by chlorination of the surface,[17] it then follows that Si etching in an HBr plasma operated under the same conditions is also limited by ion bombardment because the etch rate with HBr is slower than that with Cl_2. The ratio of the etch rate in HBr plasmas to that in Cl_2 plasmas (0.61, Table I) can be compared with the ratio of the respective halogen coverages measured after etching with these gases (0.60) and to the ratio of the respective ion fluxes (0.83), measured with the Langmuir probe. This comparison suggests that HBr plasmas etch Si more slowly than do Cl_2 plasmas mainly because less halogen is present on the surface at saturated coverage and, hence, the ion-enhanced rate of formation of volatile products such as $SiBr_2$ is lower. Since the ion fluxes are somewhat lower in HBr plasmas, the process is, however, slightly more efficient for Br on a per-halogen basis (i.e., the ratio of etch rates would be 0.83

$\times 0.60 = 0.50$ if Br and Cl were equivalent). Apparently, the 20%HBr/80%Cl_2 measurements deviate somewhat from this simple scaling relationship. Relative to a pure Cl_2 plasma, the total halogen coverage is ~5% lower and the ion flux is ~10% lower, yet the etch rate is 15% higher. While within the combined uncertainties of these measurements, secondary effects from the presence of coadsorbed H, differences in ion composition and mass, and reactions occurring in the gas phase or on the walls of the reactor could play a small role in enhancing the Si etch rate when smaller amounts (~20%) of HBr are added to Cl_2 plasmas.

Saturated chlorine coverage on photoresist surfaces is about the same as on poly-Si (Table I). Bromination in HBr-containing plasmas is different, however, in that Br coverage is less on photoresist surfaces than on Si. The Br coverage after etching photoresist in a pure HBr plasma is less than half the Cl coverage found after etching in a Cl_2 plasma (Table I). Likewise, for a mixture of 20% HBr/80%Cl_2, the Br:Cl ratio is only 0.047 on photoresist, compared to 0.11 on poly-Si. Apparently, the reduction of the etch rate of photoresist with addition of HBr to the plasma is not due to the formation of a protective brominated layer. Preferential formation of a brominated carbon layer may have been anticipated from the low vapor pressure of CBr_4 vs CCl_4. Nor is it due to the formation of an SiO_2 film in the absence of added oxygen. Instead, it is likely that Br simply reacts more slowly with the photoresist in the presence of ion bombardment, relative to H and Cl. This is consistent with the C–X bond strength (X=Br, Cl, or H) in the series $CH_3Br:CH_3Cl:CH_4 = 68:81:102$ kcal/mol.[36,37] In addition, H atoms formed in the plasma will replenish H lost from the surface of the polymer, and could reduce its etch rate by Br and Cl, in a mechanism analogous to the slowing of the etch rate of SiO_2 by the addition of O_2 to the plasma.

V. CONCLUSIONS

X-ray photoelectron spectroscopy and real-time laser desorption-laser induced fluorescence were used to study Si(100) surfaces after and during etching in HBr/Cl_2 high-density, low-pressure helical resonator plasmas. As found previously for Cl coverage on Si in Cl_2 plasmas, the Br coverage on Si, sensed by SiBr LD–LIF, did not change appreciably after the HBr plasma was extinguished and the HBr pumped away, indicating that postetching XPS analysis is indicative of the surface during etching. Br and Cl coverages on Si increase linearly with the percentage of HBr and Cl_2, respectively, in the feed gas. The Cl coverage is 1.0×10^{15} cm^{-2} after etching in a pure Cl_2 plasma, while the Br coverage is 6.0×10^{14} cm^{-2} after etching in an HBr plasma. The lower saturation coverage for Br can be ascribed to its larger atomic radius and the presence of coadsorbed H. Etch rates in pure Cl_2 plasmas are 1.6 times higher than those in HBr plasmas, in proportion to the saturated coverages of Br and Cl. These results suggest that HBr plasmas etch Si more slowly than do Cl_2 plasmas mainly because less halogen is available on the surface for formation of volatile $SiBr_x$ products in ion bombardment-stimulated reactions. The slightly lower ion fluxes in HBr plasmas, compared to Cl_2 plasmas at the same power and bias voltage, indicate that, although similar, the yield of the ion bombardment process is slightly more efficient on a per halogen basis for Br than for Cl.

The etching behavior of poly-Si is the same as Si(100). However, photoresist differs in that Br is two to three times less likely to adsorb on it than on Si vis-à-vis Cl. Apparently this at least partly explains the improvement in selectivity of Si etching relative to photoresist when HBr is added to a Cl_2 plasma. A further reduction in photoresist etch rate could be caused by hydrogenation from H atoms formed in the plasma, compensating for H lost from the resist surface as a result of ion bombardment and reactions with Cl and Br atoms.

ACKNOWLEDGMENT

Acknowledgment is made to the donors of the Petroleum Research Fund, administered by the American Chemical Society (ACS), for partial support of one of the authors (I.P.H.) in this research.

[1] D. L. Flamm, V. M. Donnelly, and D. E. Ibbotson, *VLSI Electronics Microstructure Science*, edited by N. G. Einspruch and D. M. Brown (Academic, Orlando, 1984), pp. 189–251.

[2] D. M. Manos and D. L. Flamm, *Plasma Etching, An Introduction* (Academic, Boston, 1989).

[3] H. F. Winters and J. W. Coburn, Surf. Sci. Rep. **14**, 161 (1992).

[4] D. L. Flamm, V. M. Donnelly, and J. A. Mucha, J. Appl. Phys. **52**, 3633 (1981).

[5] E. A. Ogryzlo, D. E. Ibbotson, D. L. Flamm, and J. A. Mucha, J. Appl. Phys. **67**, 3115 (1990).

[6] D. J. Oostra, R. P. van Ingen, A. Haring, and A. E. de Vries, Appl. Phys. Lett. **50**, 1506 (1987).

[7] D. X. Ma, T. A. Lin, and C. H. Chen, J. Vac. Sci. Technol. A **10**, 1217 (1992).

[8] J. F. Rembetski, Y. D. Chan, E. Boden, T. Gu, O. O. Awadelkarim, R. A. Ditizio, S. J. Fonash, X. Li, and C. R. Viswanathan, Jpn. J. Appl. Phys. **32**, 3023 (1993).

[9] K. Koshino, J. Matsuo, and M. Nakamura, Jpn. J. Appl. Phys. **32**, 3063 (1993).

[10] M. Nakamura, K. Iizuka, and H. Yano, Jpn. J. Appl. Phys. **28**, 2142 (1989).

[11] L. Y. Tsou, J. Electrochem. Soc. **136**, 3003 (1989).

[12] J. Lajzerowicz, S. Tedesco, C. Pierrat, D. Muyard, M. C. Taccussel, and P. Laporte, *Advanced Techniques for Integrated Circuit Processing*, edited by J. Bondur and T. R. Turner [Proc. SPIE **1392**, 222 (1990)].

[13] D. E. Ibbotson and C. P. Chang, in *Dry Etch Technology*, edited by D. Ranadive [Proc. SPIE **1593**, 130 (1991)].

[14] H. L. Denton and R. M. Wallace, in *Advanced Techniques for Integrated Circuit Processing II*, edited by J. Bondur, G. Castleman, L. R. Harriott, and T. R. Turner [Proc. SPIE **1803**, 36 (1992)].

[15] C. C. Cheng, K. V. Guinn, and V. M. Donnelly, J. Vac. Sci. Technol. B (submitted).

[16] I. P. Herman, V. M. Donnelly, K. V. Guinn, and C. C. Cheng, Phys. Rev. Lett. **72**, 2801 (1994).

[17] C. C. Cheng, K. V. Guinn, V. M. Donnelly, and I. P. Herman, J. Vac. Sci. Technol. A **12**, 2630 (1994).

[18] K. V. Guinn and V. M. Donnelly, J. Appl. Phys. **75**, 2227 (1994).

[19] K. V. Guinn, C. C. Cheng, and V. M. Donnelly, J. Vac. Sci. Technol. B **13**, 214 (1995).

[20] (a) Due to a pressure drop that was not properly accounted for, the pressure of 1.0 mTorr given in previous studies (Refs. 16–18) was actually the same as the correct pressure of 2.1 mTorr used in this study. Similarly, the quoted pressures below 1.0 mTorr in Ref. 17 should be multiplied by 2, while those above ~5 mTorr are correct. (b) Br($3d$) was used, rather than Br($3p$) because its spin-orbit splitting is smaller, resulting in a sharper peak. In addition, the baseline is flatter in the Br($3d$) region. A loss feature associated with Si($2s$) overlaps with the Br($3p$) lines, making an accurate peak integration difficult. The 15% higher apparent Br coverages calculated using the Br($3p$) peaks can be mostly attributed to this artifact.

[21] H. Feil, J. Dieleman, and B. J. Garrison, J. Appl. Phys. **74**, 1303 (1993); J. Dieleman, F. H. M. Sanders, A. W. Kolfschoten, P. C. Zalm, A. E. de Vries, and A. Haring, J. Vac. Sci. Technol. B **3**, 1384 (1985).
[22] K. P. Huber and G. Herzberg, *Constants of Diatomic Molecules* (Van Nostrand Reinhold, New York, 1979).
[23] *Spectroscopic Data*, Heteronuclear Diatomic Molecules, Vol. 1, edited by S. N. Suchard (Plenum, New York, 1975), Pt. B, p. 985.
[24] P. Gupta, P. A. Coon, B. G. Koehler, and S. M. George, Surf. Sci. **249**, 92 (1991).
[25] A. Aliouchouche, J. Boulmer, B. Bourguignon, J.-P. Budin, D. Debarre, and A. Desmur, Appl. Surf. Sci. **69**, 52 (1993).
[26] J. Boulmer, B. Bourguignon, J.-P. Budin, and D. Debarre, Appl. Surf. Sci. **43**, 424 (1989).
[27] J. Boulmer, B. Bourguignon, J.-P. Budin, and D. Debarre, Chemtronics **4**, 165 (1989).
[28] J. Boulmer, B. Bourguignon, J.-P. Budin, D. Debarre, and A. Desmur, J. Vac. Sci. Technol. A **9**, 2923 (1991).
[29] R. DeJonge, J. Majoor, K. Benoist, and D. DeVries, Europhys. Lett. **2**, 843 (1986).
[30] C. C. Cheng, Q. Gao, W. J. Choyke, and J. T. Yates, Jr., Phys. Rev. B, **46**, 12810 (1992).
[31] Q. Gao, C. C. Cheng, P. J. Chen, W. J. Choyke, and J. T. Yates, Jr., J. Chem. Phys. **98**, 8308 (1993).
[32] J. Matsuo, F. Yannick, and K. Karahashi, Surf. Sci. **283**, 52 (1993).
[33] K. Karahashi, J. Matsou, and S. Hijija, Appl. Surf. Sci. **60/61**, 126 (1992).
[34] D. D. Koleske and S. M. Gates, J. Chem. Phys. **99**, 8218 (1993).
[35] R. B. Jackman, R. J. Price, and J. S. Foord, Surf. Sci. **36**, 296 (1989).
[36] I. Barin, O. Knacke, and O. Kubaschewski, *Thermodynamical Properties of Inorganic Substances*, 1977 Supplement (Springer, Berlin, 1973).
[37] JANAF *Thermochemical Tables* (1985).